Binuclear Cyclometalated Platinum(II) 4,6-Diphenyl-2,2′-bipyridine Complexes: Interesting Photoluminescent and Optical Limiting Materials

Wenfang Sun,* Hongjun Zhu, and Paul M. Barron

Department of Chemistry and Molecular Biology, North Dakota State University, Fargo, North Dakota 58105

Received January 21, 2006. Revised Manuscript Received March 11, 2006

The UV−vis spectra, emission spectra and lifetimes, transient absorption characteristics, and optical limiting performances of three binuclear cyclometalated platinum(II) 4,6-diphenyl-2,2′-bipyridine complexes with bis(diphenylphosphino)methane (dppm), bis(diphenylphosphino)ethane (dppe), and bis-(diphenylphosphino)propane (dppp) bridging ligands have been investigated. All three complexes exhibit concentration-dependent photoluminescence in CH_3CN at room temperature and 77 K, and the emission energy is affected by the length of the bridging ligand. $[Pt_2L_2(\mu\text{-dppm})](ClO_4)_2$ (**1**) (L = 4,6-diphenyl-2,2′-bipyridine) shows a broad, structureless emission band at about 667 nm when the complex concentration is higher than 6.0×10^{-5} mol/L, which can be attributed to a $^3[d\sigma^*,\pi^*]$ state due to metal−metal interactions. $[Pt_2L_2(\mu\text{-dppe})](ClO_4)_2$ (**2**) and $[Pt_2L_2(\mu\text{-dppp})](ClO_4)_2$ (**3**) essentially exhibit no metal−metal interactions between the two platinum centers, and their emission can be ascribed to a ^{3}MLCT (metal-to-ligand charge transfer) excited state. The emission lifetime is approximately 200 ns for **1** at 1.2×10^{-4} mol/L, ∼1.5 μs for **2** at 1.4×10^{-4} mol/L, and ∼2.0 μs (68%) and ∼0.4 μs (32%) for **3** at 1.3×10^{-4} mol/L. All complexes show moderately intense, broad positive transient difference absorption bands from near-UV and extending to near-IR spectral regions. The nonlinear transmission experiment at 532 nm using 4.1 ns laser pulses demonstrates that **2** and **3** exhibit stronger optical limiting for nanosecond laser pulses than SiNc, which is likely associated with their very low ground-state absorption cross sections and relatively long triplet excited-state lifetimes (approximately microseconds).

Introduction

The photophysics of a variety of mononuclear square-planar platinum(II) complexes have been studied extensively in recent years because of their potential applications in chemosensors,[1] light emitting devices,[2] photovoltaic cells,[3] and photocatalysis.[4] Our group recently reported the potential use of mononuclear terdentate platinum(II) complexes as third-order nonlinear optical materials.[5] These complexes exhibit high linear transmission at low incident fluences but strong reverse saturable absorption at high incident fluences over a broad visible to near-infrared spectral region, making them promising candidates for broadband optical limiting application. However, the photochemistry of binuclear platinum(II) complexes is more appealing because the origin of the lowest excited state can be tuned by the extent of metal−metal interactions between the diplatinum centers, which in turn results in unusual colors and long-wavelength emission.[6] Earlier studies on the binuclear platinum(II) complexes have only been focused on the luminescence properties of the complexes;[6] no third-order nonlinear optical properties of

* Corresponding author. E-mail: wenfang.sun@ndsu.edu. Phone: 701-231-6254. Fax: 701-231-8831.

(1) (a) Kunugi, Y.; Mann, K. R.; Miller, L. L.; Exstrom, C. L. *J. Am. Chem. Soc.* **1998**, *120*, 589. (b) Exstrom, C. L.; Sowa, J. R.; Daws, C. A.; Janzen, D. E.; Mann, K. R. *Chem. Mater.* **1995**, *7*, 15. (c) Daws, C. A.; Exstrom, C. L.; Sowa, J. R.; Mann, K. R. *Chem. Mater.* **1997**, *9*, 363. (d) Lee, W. W. S.; Wong, K. Y.; Li, X. M. *Anal. Chem.* **1993**, *65*, 255. (e) Wu, L. Z.; Cheung, T. C.; Che, C. M.; Cheung, K. K.; Lam, M. H. W. *Chem. Commun.* **1998**, 1127. (f) Yang, Q.-Z.; Wu, L.-Z.; Zhang, H.; Chen, B.; Wu, Z.-X.; Zhang, L.-P.; Tung, Z.-H. *Inorg. Chem.* **2004**, *43*, 5195. (g) Wong, K. M.-C.; Tang, W.-S.; Lu, X.-X.; Zhu, N.; Yam, V. W.-W. *Inorg. Chem.* **2005**, *44*, 1492.

(2) (a) Adamovich, V.; Brooks, J.; Tamayo, A.; Alexander, A. M.; Djurovich, P. I.; D'Andrade, B. W.; Adachi, C.; Forrest, S. R.; Thompson, M. E. *New J. Chem.* **2002**, *26*, 1171. (b) Lin, Y. Y.; Chan, S. C.; Chan, M. C. W.; Hou, Y. J.; Zhu, N.; Che, C. M.; Liu, Y.; Wang, Y. *Chem.—Eur. J.* **2003**, *9*, 1263. (c) Lu, W.; Mi, B. X.; Chan, M. C. W.; Hui, Z.; Che, C. M.; Zhu, N.; Lee, S. T. *J. Am. Chem. Soc.* **2004**, *126*, 4958. (d) Kwok, C.-C.; Ngai, H. M. Y.; Chan, S.-C.; Sham, I. H. T.; Che, C.-M.; Zhu, N. *Inorg. Chem.* **2005**, *44*, 4442.

(3) (a) McGarrah, J. E.; Kim, Y.-J.; Hissler, M.; Eisenberg, R. *Inorg. Chem.* **2001**, *40*, 4510. (b) Islam, A.; Sugihara, H.; Hara, K.; Singh, L. P.; Katoh, R.; Yanagida, M.; Takahashi, Y.; Murata, S.; Arakawa, H. *Inorg. Chem.* **2001**, *40*, 5371. (c) McGarrah, J. E.; Eisenberg, R. *Inorg. Chem.* **2003**, *42*, 4355.

(4) (a) Connick, W. B.; Gray, H. B. *J. Am. Chem. Soc.* **1997**, *119*, 11620. (b) Hissler, M.; McGarrah, J. E.; Connick, W. B.; Geiger, D. K.; Cummings, S. D.; Eisenberg, R. *Coord. Chem. Rev.* **2000**, *208*, 115. (c) Zhang, D.; Wu, L.-Z.; Zhou, L.; Han, X.; Yang, Q.-Z.; Zhang, L.-P.; Tung, C.-H. *J. Am. Chem. Soc.* **2004**, *126*, 3440.

(5) (a) Sun, W.; Wu, Z.-X.; Yang, Q.-Z.; Wu, L.-Z.; Tung, C.-H. *Appl. Phys. Lett.* **2003**, *82*, 850. (b) Guo, F.; Sun, W.; Liu, Y.; Schanze, K. *Inorg. Chem.* **2005**, *44*, 4055. (c) Sun, W.; Guo, F. *Chin. Opt. Lett.* **2005**, *S3*, S34.

(6) (a) Yip, H.-K.; Che, C.-M.; Zhou, Z.-Y.; Mak, T. C. W. *J. Chem. Soc. Chem. Commun.* **1992**, 1369. (b) Bailey, J. A.; Miskowski, V. M.; Gray, H. B. *Inorg. Chem.* **1993**, *32*, 369. (c) Wu, L.-Z.; Cheung, T.-C.; Che, C.-M.; Cheung, K.-K.; Lam, M. H. W. *Chem. Commun.* **1998**, 1127. (d) Lai, S.-W.; Chan, M. C.-W.; Cheung, T.-C.; Peng, S.-M.; Che, C.-M. *Inorg. Chem.* **1999**, *38*, 4046. (e) Lu, W.; Chan, M. C. W.; Zhu, N.; Che, C.-M.; Li, C.; Hui, Z. *J. Am. Chem. Soc.* **2004**, *126*, 7639. (f) Ma, B.; Li, J.; Djurovich, P. I.; Yousufuddin, M.; Bau, R.; Thompson, M. E. *J. Am. Chem. Soc.* **2005**, *127*, 28. (g) Cheung, T.-C.; Cheung, K.-K.; Peng, S.-M.; Che, C.-M. *J. Chem. Soc., Dalton Trans.* **1996**, 1645.

10.1021/cm060161n CCC: $33.50
Published on Web 04/15/2006

these complexes have been reported. In addition, for bis(diphenylphosphino)alkane bridged binuclear platinum(II) complexes with a 6-phenyl-2,2′-dipyridine ligand, only the complexes with bis(diphenylphosphino)methane (dppm) and bis(diphenylphosphino)propane (dppp) bridging ligands have been reported by Che and co-workers.[6d,g] It is found that emissions from the complexes with the dppm bridging ligand red-shift significantly as a result of the interactions between the two platinum centers,[6d,g] while the complex with the dppp bridge shows essentially no metal−metal interactions and thus the emission is similar to that of its mononuclear congener.[6d] These results are interesting; however, no study has been reported on the complex with a bis(diphenylphosphino)ethane (dppe) bridging ligand. It is unknown whether such a complex possesses characteristics transitional between the dppm bridged complex and the dppp bridged complex. To remedy this deficiency and to understand the effect of metal−metal coupling on nonlinear optical properties of the binuclear platinum complexes, a new binuclear platinum(II) 4,6-diphenyl-2,2′-bipyridine (dphbpy) complex with a dppe bridging ligand has been synthesized. The electronic absorption, photoluminescence, excited-state absorption characteristics, and optical limiting performance of this complex have been investigated and reported in this paper. For comparison of the extent of metal−metal coupling, binuclear platinum(II) dphbpy complexes with dppm and dppp bridging ligands have also been synthesized and studied.

Experimental Section

Synthesis. The dphbpy ligand and its platinum(II) chloride complex, as well as the binuclear cyclometalated platinum(II) dphbpy complexes with dppm, dppe, and dppp bridging ligands were synthesized according to literature procedures.[6d,7] Except for $[Pt_2L_2(\mu\text{-dppm})](ClO_4)_2$ (**1**) (L = dphbpy) that has been reported in the literature,[6d] $[Pt_2L_2(\mu\text{-dppe})](ClO_4)_2$ (**2**) and $[Pt_2L_2(\mu\text{-dppp})](ClO_4)_2$ (**3**) are new complexes, and the characterization data are provided in the following. 1-Phenacylpyridinium bromide, dppm, dppe and dppp were purchased from Aldrich Chemical Co. 2-Acetylpyridine, benzaldehyde, and potassium tetrachloroplatinate were obtained from Alfa Aesar. All solvents purchased from VWR Scientific Products were analytical grade and were used directly for synthesis without further purifications.

The synthesized compounds were characterized using ^{1}H NMR, electrospray ionization high-resolution mass spectrometry (ESI-HRMS), and elemental analyses. ^{1}H NMR spectra were measured on a Varian 400 MHz VNMR spectrometer. ESI-HRMS analyses were conducted on a Bruker Daltonics BioTOF III mass spectrometer. Elemental analyses were performed on a Perkin-Elmer 2400 Series II CHNS/O analyzer.

1. ^{1}H NMR (DMSO-d_6) δ: 5.22 (broad t, 2H), 6.15 (s, 2H), 6.40−6.45 (m, 2H), 6.58−6.70 (m, 6H), 7.34−7.60 (m, 20H), 7.76−7.80 (m, 8H), 7.95−8.04 (m, 4H), 8.22 (s, 2H), 8.38−8.50 (m, 6H). ESI-MS: *m*/*z* calcd for $[C_{69}H_{52}N_4P_2Pt_2^{194}]^{2+}$, 693.1456; found, 693.1490 (23%); calcd for $[C_{69}H_{52}N_4P_2Pt_2^{195}]^{2+}$, 694.1475; found, 694.1501 (100%); calcd for $[C_{69}H_{52}N_4P_2Pt_2^{196}]^{2+}$, 695.1492; found, 695.1509 (71%). Anal. Calcd for $C_{69}H_{52}N_4P_2Pt_2Cl_2O_8\cdot 3H_2O$: C, 50.46; H, 3.56; N, 3.41. Found: C, 50.62; H, 3.45; N, 3.38.

2. ^{1}H NMR (DMSO-d_6) δ: 3.85 (broad, 4H), 5.80 (m, 2H), 6.10−6.22 (m, 2H), 6.54−6.58 (m, 2H), 6.95−7.02 (m, 2H), 7.07−7.19 (m, 4H), 7.39−7.52 (m, 10H), 7.55−7.58 (m, 4H), 7.62−7.68 (m, 4H), 7.72−7.77 (m, 4H), 7.83−8.06 (m, 14H), 8.08−8.14 (m, 2H). ESI-MS: *m*/*z* calcd for $[C_{70}H_{54}N_4P_2Pt_2^{194}]^{2+}$, 700.1542; found, 700.1591 (26%); calcd for $[C_{70}H_{54}N_4P_2Pt_2^{195}]^{2+}$, 701.1562; found, 701.1607 (100%); calcd for $[C_{70}H_{54}N_4P_2Pt_2^{196}]^{2+}$, 702.1564; found, 702.1611 (73%). Anal. Calcd for $C_{70}H_{54}N_4P_2Pt_2Cl_2O_8\cdot H_2O$: C, 51.89; H, 3.48; N, 3.46. Found: C, 51.59; H, 3.38; N, 3.50.

3. ^{1}H NMR (DMSO-d_6) δ: 3.15−3.25 (broad, 2H), 3.40−3.45 (m, 4H), 6.25−6.28 (m, 2H), 6.33−6.35 (m, 2H), 6.61−6.64 (m, 2H), 6.80−6.81 (m, 2H), 6.92−6.95 (m, 2H), 7.23−7.25 (m, 2H), 7.40−7.42 (m, 8H), 7.48−7.49 (m, 4H), 7.54−7.56 (m, 4H), 7.60−7.61 (m, 2H), 7.68 (s, 2H), 7.75−7.80 (m, 12H), 7.93−7.96 (m, 2H), 8.03 (s, 2H), 8.12−8.14 (m, 2H). ESI-MS: *m*/*z* calcd for $[C_{71}H_{56}N_4P_2Pt_2^{194}]^{2+}$, 707.1612; found, 707.2102 (24%); calcd for $[C_{71}H_{56}N_4P_2Pt_2^{195}]^{2+}$, 708.1632; found, 708.21261 (100%); calcd for $[C_{71}H_{56}N_4P_2Pt_2^{196}]^{2+}$, 709.1649; found, 709.2130 (74%). Anal. Calcd for $C_{71}H_{56}N_4P_2Pt_2Cl_2O_8$: C, 52.76; H, 3.49; N, 3.47. Found: C, 52.56; H, 3.56; N, 3.35.

Photophysical Measurement. UV−vis spectra were obtained using a CARY 500 Dual Beam Scanning UV−vis−near-IR spectrophotometer. Steady emission and excitation spectra at room temperature and 77 K were measured on a SPEX Fluorolog-3 fluorimeter/phosphorimeter. The excitation wavelength was 355 nm for all of the samples unless otherwise noted. The solutions were purged with argon for 30 min before each measurement. The time-resolved emission spectra, the lifetimes of emission, and the triplet transient difference absorption spectra and lifetimes were measured on an Edinburgh LP920 laser flash photolysis spectrometer. The samples were excited by the third harmonic output (355 nm) of a Quantel Brilliant Nd:YAG laser; the laser pulse width (fwhm) was 4.1 ns, and the repetition rate was adjusted to 1 Hz for emission measurements and 3.3 Hz for transient absorption measurements.

Optical Limiting Measurement. Optical limiting measurements were carried out at 532 nm using a 4.1 ns Quantel Nd:YAG laser. The experimental setup is similar to the one described previously,[5b] with a 30-cm focal length lens focusing the beam waist to ∼66 μm (radius) to the center of a 2-mm sample cuvette. The complex concentration was adjusted to afford the same linear transmission of 76% at 532 nm in the 2-mm cuvette. Two Molectron J4-09 pyroelectric probes and a EPM2000 energy/power meter were used to monitor the incident and output energies.

Results and Discussion

Electronic Absorption Spectra. Figure 1a shows the UV−vis absorption spectra of complexes **1**−**3** in acetonitrile solutions at concentrations of $1.2-1.4 \times 10^{-4}$ mol/L. All three complexes exhibit similar features in the UV region, which can be assigned to the intraligand $^1\pi,\pi^*$ transition.[6d] However, the spectra of **2** and **3** in the visible region are quite distinct from that of **1**. For complex **1**, a broad, moderately intense band presents above 400 nm that can be assigned to the $^1[d\sigma^*,\pi^*]$ transition due to metal−metal interactions.[6d,g] The absorption band maxima and the molar extinction coefficients for **1** are in accordance with the reported data.[6d] In contrast, such a broad band is absent in the spectra of **2** and **3**, except **2** shows a weak shoulder at 510 nm. This indicates that no or very weak metal−metal interactions are evident in these two complexes, which could be attributed to the longer carbon chains between the

(7) (a) Kröhnke, F. *Synthesis* **1976**, 1. (b) Kröhnke, F.; Zecher, W.; Curtze, J.; Drechsler, D.; Pfleghar, K.; Schnalke, K. E.; Weis, W. *Angew. Chem., Int. Ed. Engl.* **1962**, *1*, 626.

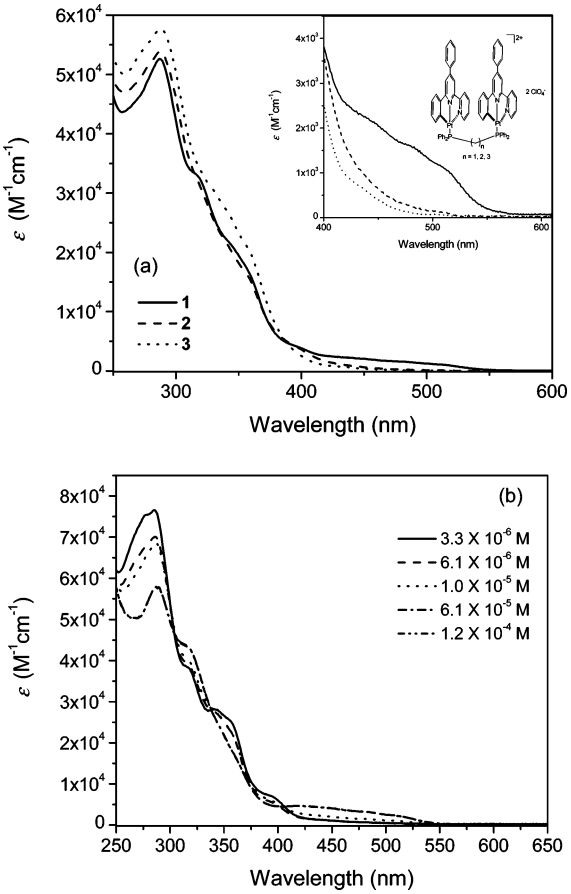

Figure 1. (a) Chemical structure and UV−vis spectra of binuclear platinum(II) complexes $[Pt_2L_2(\mu\text{-dppC}_n)](ClO_4)_2$ in CH_3CN at a concentration of 1.2×10^{-4} mol/L for **1**, 1.4×10^{-4} mol/L for **2**, and 1.3×10^{-4} mol/L for **3**. (b) UV−vis spectra of **1** at different concentrations. The spectra at 6.1×10^{-5} mol/L and 1.2×10^{-4} mol/L overlap.

phosphorus atoms that leads to greater separations between the two [PtL] moieties. Hence, the two [PtL] fragments in **2** and **3** behave like discrete noninteracting moieties, giving rise to absorption spectra resembling that of the mononuclear triphenylphosphine counterpart.[6d,g] In addition, these absorption spectra are essentially transparent above 550 nm, providing a broad optical window in the visible to near-infrared region, in which optical limiting may occur.[8]

An interesting feature noticed during the UV−vis spectral study is the concentration-dependent profile for these complexes. As demonstrated in Figure 1b for **1**, when the concentration of the solution is lower than 6×10^{-5} mol/L, the maximum of the absorption band in the UV region gradually red-shifts with increased concentration, accompanied by a decrease of the molar extinction coefficient and a disappearance of some vibronic structures. Instead, the molar extinction coefficient for the shoulder around 316 nm increases, and a broad band above 400 nm appears. All these features imply that dimerization or oligomerization occurs when the concentration is increased. However, the spectrum becomes steady when the concentration is higher than 6×10^{-5} mol/L. No further change is observed even when the solution concentration is increased to 5×10^{-4} mol/L. This

(8) Perry, J. W.; Mansour, K.; Lee, I.-Y. S.; Wu, X.-L.; Bedworth, P. V.; Chen, C.-T.; Ng, D.; Marder, S. R.; Miles, P.; Wada, T.; Tian, M.; Sasabe, H. *Science* **1996**, *273*, 1533.

Table 1. Photophysical Parameters for Complexes 1−3 in Acetonitrile

complex	UV−vis[a] λ_{max}, nm (ϵ, dm^3 mol^{-1} cm^{-1})	emission[a] λ_{max}, nm (τ, ns) at 298 K	emission[a] λ_{max}, nm (τ, ns) at 77 K	TA[b] λ_{max}, nm (τ, ns) at 298 K
1	287 (52600), 316 (33200), 344 (21200), 358 (16700), 420 (2600), 482 (1600), 510 (1100)	640 (204), 667 (202)	637 (2370, 89%; 193, 11%)	380 (175); 590 (184)
2	287 (53900), 356 (16500), 427 (1300), 510 (110)	544 (1497), 591 (1476)	534 (3409, 92%; 313, 8%), 581 (3456, 94%; 271, 6%)	385 (1822); 571 (1784)
3	288 (57700), 334 (29100), 358 (20500), 434 (690), 500 (60)	544 (1961, 68%; 390, 32%)	521 (8238, 96%; 573, 4%), 558 (8259, 95%; 668, 5%)	390 (1854, 71%; 388, 29%), 536 (2031, 74%; 380, 26%)

[a] Measured at a complex concentration of 1.2×10^{-4} mol/L for **1**, 1.4×10^{-4} mol/L for **2**, and 1.3×10^{-4} mol/L for **3**. [b] Complex concentration is 2.7×10^{-5} mol/L for **1**, 3.2×10^{-5} mol/L for **2**, and 1.9×10^{-5} mol/L for **3**.

indicates that a stable form of aggregates forms at higher concentrations. A similar concentration-dependent feature has been observed for **2** and **3**, but without the appearance of the broad $^1[d\sigma^*,\pi^*]$ band above 400 nm. This suggests that the dimerization may occur intramolecularly rather than intermolecularly. Our hypothesis is that, at a low concentration, the complex may adopt a *trans* conformation, showing no metal−metal/$\pi-\pi$ interactions, which is supported by the similarity of the UV−vis spectra of these three complexes at a low concentration of 6×10^{-6} mol/L. At a higher concentration, the conformation of the complex could adjust to *cis* to reduce the crowd. As a result of the different lengths of the bridging ligand in these three complexes, the distance between the two [PtL] moieties varies, resulting in the different metal−metal separation. The conformational transformation may be complete at the concentration of 6×10^{-5} mol/L, evidenced by the appearance of a steady UV−vis spectrum. The molar extinction coefficients presented in Table 1 for these three complexes are extrapolated from the spectra corresponding to complex concentrations of $1.2-1.4 \times 10^{-4}$ mol/L.

Emission Data. All three complexes are emissive at room temperature in solution and at 77 K in glassy solution. As shown in Figure 2 and Table 1, the emission band maxima for these complexes in acetonitrile at room temperature are influenced drastically by the bridging ligand. At a similar concentration of $1.2-1.4 \times 10^{-4}$ mol/L, **1** emits at 667 nm (max) with a shoulder at about 640 nm, which is consistent with the literature report.[6d] For **2**, a broad emission band is seen at about 591 nm with a shoulder at ~544 nm. In contrast, **3** emits at 544 nm. Similar to the UV−vis spectra, the emission energy also reflects the effects of distance and interactions between the two [PtL] units. According to earlier work reported by Che and co-workers, the emitting state for **1** can be assigned to a $^3[d\sigma^*,\pi^*]$ excited state due to the

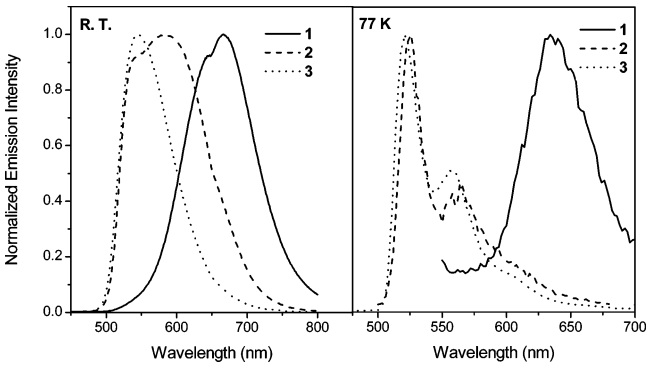

Figure 2. Normalized emission spectra of **1**−**3** in acetonitrile at room temperature and 77 K ($\lambda_{ex} = 355$ nm). The complex concentration is 1.2×10^{-4} mol/L for **1**, 1.4×10^{-4} mol/L for **2**, and 1.3×10^{-4} mol/L for **3**.

close distance and interactions between the two platinum centers.[6d,g] For **3**, the emission energy resembles that of the mononuclear triphenylphosphine relative,[6d,g] suggesting that the two [PtL] units behave like two discrete moieties. Therefore, the emitting state for **3** can be ascribed to a triplet metal-to-ligand charge transfer (^{3}MLCT) state, similar to that of the mononuclear congener[6d,g] and its 6-phenyl-2,2′-dipyridine binuclear platinum(II) analogue.[6d] For **2**, the emission spectrum is strikingly different, with a very broad, somewhat structured feature. The shoulder at 544 nm is similar to the emission maxima for **3**, and the mononuclear triphenylphosphine complex, hence, can be assigned as ^{3}MLCT in nature as well. The low-energy maximum at 591 nm shows a similar decay rate and excitation spectrum as those of the emission at about 544 nm, suggesting that this band could originate from the same excited state, that is, the ^{3}MLCT excited state. The appearance of such a low-energy band in **2** but not in **3** is presumably attributed to the reduced separation between the two [PtL] units in **2** compared to that in **3**, which gives rise to intramolecular $\pi-\pi$ interactions.

At 77 K, the emission bands blue-shift for all three complexes. For glassy solution with a concentration of $1.2-1.4 \times 10^{-4}$ mol/L, **1** exhibits a structureless emission at about 637 nm that can be attributed to the ^{3}[dσ*,π*] excited state.[6d,g] **2** and **3** show vibronic structures with a spacing of about 1100 cm^{-1}. Such vibronic progression spacing corresponds to the aromatic vibrational mode of the terdentate ligand[9] and is consistent with that of the mononuclear triphenylphosphine counterpart. Therefore, the emission for **2** and **3** at 77 K is tentatively assigned to a ^{3}MLCT excited state.[6d,g] Similar to the trend observed from the UV−vis spectra and the emission at room temperature, the emission at 77 K also reflects the distance and interactions between the two [PtL] units. With the increased bridging length, the intramolecular interactions between the two [PtL] units become weaker, resulting in the changes of the origin of emitting state and the emission energy.

Similar to the UV−vis spectra, the emissions of **1** and **2** exhibit drastic concentration dependence at both room temperature and 77 K. At room temperature, as shown in Figure 3, when the concentration is lower than 1.0×10^{-5} mol/L, both of them emit at about 550 nm, resembling that of the mononuclear platinum(II) triphenylphosphine complex, and can be assigned to ^{3}MLCT in nature.[6d,g] The emission maximum red-shifts at higher concentration ($>6.0 \times 10^{-5}$ mol/L), appearing at about 667 nm (max) for **1** and 591 nm (max) for **2** with a shoulder at 544 nm. The excitation spectrum monitored at 667 nm for **1** shows a broad band in

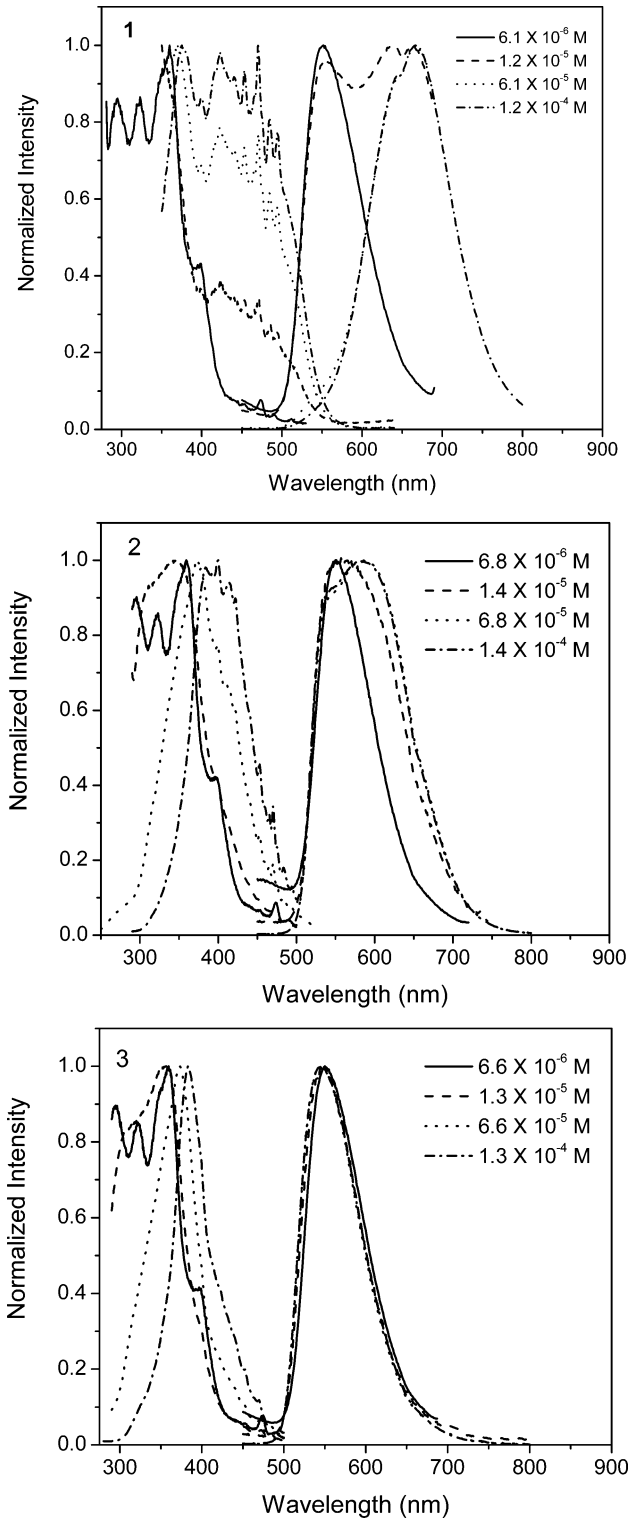

Figure 3. Normalized emission (shown in the right side of the figure, $\lambda_{ex} = 355$ nm) and excitation (shown in the left side of the figure, monitored at emission maximum) spectra of **1**−**3** at different concentrations in acetonitrile at room temperature. The emission spectra at $6.1-6.8 \times 10^{-5}$ mol/L and $1.2-1.4 \times 10^{-4}$ mol/L overlap.

(9) Yam, V. W.-W.; Tang, R. P.-L.; Wong, K. M.-C.; Cheung, K.-K. *Organometallics* **2001**, *20*, 4476.

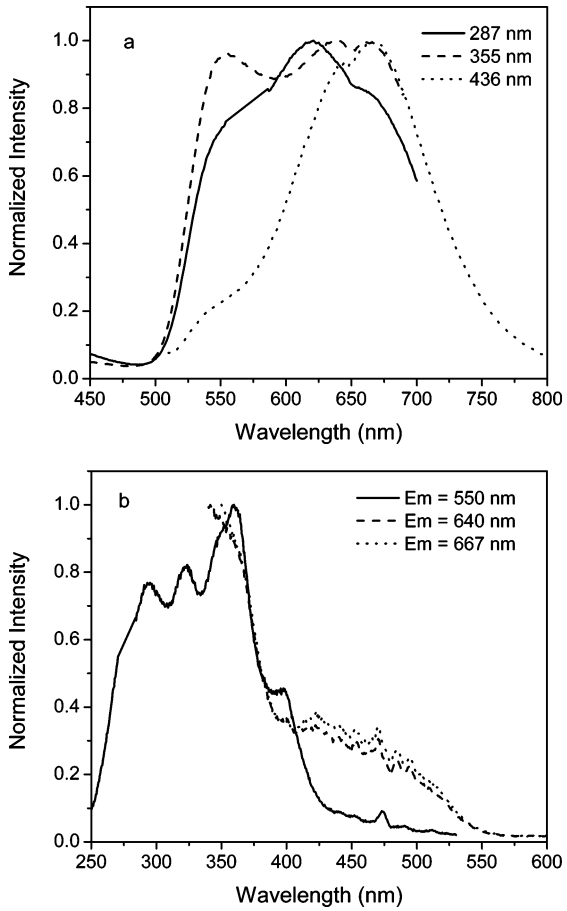

Figure 4. Normalized emission (a) and excitation (b) spectra of **1** monitored at different excitation and emission wavelengths at a complex concentration of 1.2×10^{-5} mol/L at room temperature.

the region of 400−550 nm (Figure 4b), which is consistent with the [dσ*,π*] transition evident in the UV−vis spectrum. Apparently, the emitting state changes from ^{3}MLCT to ^{3}[dσ*,π*] at higher concentration for **1**, which is further evident from the emission lifetime change that is listed in Table 2 and will be discussed later. For **2**, although virtually no metal−metal interactions are evident at high concentration from the UV−vis, excitation, or emission spectra, the presence of intramolecular $\pi-\pi$ interactions are feasible, as reflected by the appearance of a low-energy emission at 591 nm (tentatively assigned to an intramolecular excimer emission), a shoulder around 510 nm in the UV−vis spectrum, and a broad band in the region of 400−500 nm in the excitation spectrum. At an intermediate concentration ($1.2-1.4 \times 10^{-5}$ mol/L), the emission exhibits characteristics that are transitional between noninteracting and interacting species, with three bands appearing at 550, 644, and 668 nm for **1** and one broad band at about 570 nm for **2**. The emission of **1** at 1.2×10^{-5} mol/L exhibits excitation wavelength dependence. As shown in Figure 4, upon excitation at 287 nm, the emission is dominated by the 620 nm peak, with two shoulders appearing at about 550 and 667 nm. When excited at 355 nm, three bands corresponding to ^{3}MLCT parentage (at 550 nm) and ^{3}[dσ*,π*] origin (640 and 667 nm) appear. Excitation at 436 nm gives rise to the ^{3}[dσ*,π*] dominated emission. This site-selective emission suggests the presence of multiple emitting species in the solution, presumably as a result of the presence of different conformers at this complex concentration. Consistent with this notion, the excitation spectra of **1** monitored at 640 and 667 nm (Figure 4b) is distinct from that monitored at 550 nm, indicating the different origin of the emission band at 550 nm and those at 640 and 667 nm. The appearance of the broad band in the region of 400−550 nm when monitored at 640 and 667 nm emission bands is in line with the feature observed in the UV−vis spectra at this concentration, confirming the presence of the intramolecularly interacting conformer (*cis*) that gives rise to the [dσ*,π*] transition. However, such a concentration-dependent emission feature disappears when the complex concentration is higher than 6.0×10^{-5}, implying the appearance of a steady, uniform

Table 2. Emission and TA Data for Complexes 1−3 at Different Concentrations in Acetonitrile

complex	concentration (mol/L)	emission λ_{max}, nm (τ, ns) at 298 K	emission λ_{max}, nm (τ, ns) at 77 K	TA λ_{max}, nm (τ, ns) at 298 K
1	6.1×10^{-6}	550 (54)	512, 544	380 (56), 590 (55)
	1.2×10^{-5}	550 (56), 644 (49, 15%; 178, 85%), 668 (167)	517 (2227, 79%; 172, 21%), 538 (2424, 62%; 210, 38%), 637 (3508, 93%; 196, 7%)	380 (63), 590 (87)
	6.1×10^{-5}	644 (207), 668 (207)	637 (1944, 92%; 128, 8%)	380 (172), 590 (180)
	1.2×10^{-4}	640 (204), 667 (202)	637 (2370, 89%; 193, 11%)	380 (175), 590 (184)
2	6.8×10^{-6}	550 (57)	468	385 (65), 571 (58)
	1.4×10^{-5}	570 (1693, 93%; 64, 7%)	468 (138, 69%; 13, 31%), 497 (142, 72%; 12, 28%)	385 (72), 571 (67)
	6.8×10^{-5}	542 (1695), 586 (1739)	531 (3816, 96%; 205, 4%), 570 (3928, 94%; 290, 6%)	385 (1454), 571 (1496)
	1.4×10^{-4}	544 (1497), 591 (1476)	534 (3409, 92%; 313, 8%), 581 (3456, 94%; 271, 6%)	385 (1822), 571 (1784)
	5.1×10^{-4}	544 (1202), 591 (1277)	539 (2867, 88%; 378, 12%), 590 (3737, 93%; 423, 7%)	571 (1141)
3	6.6×10^{-6}	550 (58)	465, 494	390 (55), 536 (49)
	1.3×10^{-5}	548 (718, 76%; 79, 24%)	465 (211, 32%; 16, 68%), 494	390 (790, 84%; 77, 16%), 536 (694, 78%; 85, 22%)
	6.6×10^{-5}	544 (1529, 63%; 316, 37%)	529 (6795, 93%; 396, 7%), 562 (6091, 93%; 320, 7%)	390 (1420, 71%; 284, 29%), 536 (1550, 75%; 265, 25%)
	1.3×10^{-4}	544 (1961, 68%; 390, 32%)	521 (8238, 96%; 573, 4%), 558 (8259, 95%; 668, 5%)	390 (1854, 71%; 388, 29%), 536 (2031, 74%; 380, 26%)

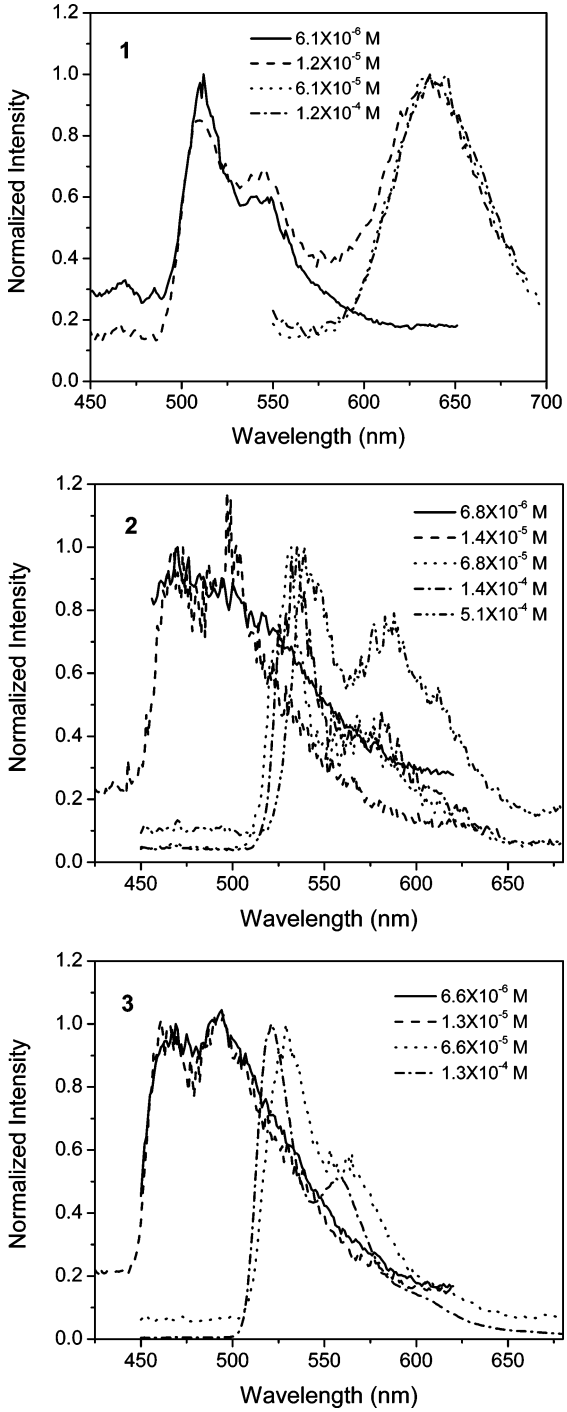

Figure 5. Normalized emission spectra of **1**−**3** at different concentrations in CH_3CN at 77 K (λ_{ex} = 355 nm).

species in the solution. The concentration-dependent emission feature of **1** and **2** is in accordance with that of a trinuclear C^N^N platinum(II) complex tethered by oligophosphine auxiliaries reported by Che and co-workers,[6e] although the authors attributed such a feature to dimerization or oligomerization. In contrast to **1** and **2**, the emission of **3** only exhibits a slight blue shift when the complex concentration is increased, which is similar to that of the mononuclear triphenylphosphine complex (dphbpyPtPPh$_3$·ClO$_4$).

At 77 K, as shown in Figure 5, the emission appears at higher energies for all three complexes when the concentration is approximately 6.0×10^{-6} mol/L, with **1** emitting at 512 nm with a shoulder at 544 nm, **2** showing a structureless broad band at about 468 nm, and **3** exhibiting two identically intense bands at 465 and 494 nm. At the concentration of $1.2-1.4 \times 10^{-5}$ mol/L, a broad structureless band appears at about 637 nm in addition to the structured bands at 512 and 544 nm for **1**. For **2**, the broad band at lower concentration splits into two bands at 468 and 497 nm with almost identical intensity. No pronounced shift was found for **3** at a similar concentration (1.3×10^{-5} mol/L) in comparison to that of lower concentration (6.6×10^{-6} mol/L). However, when the concentration is higher than 6.0×10^{-5} mol/L, the emission shows a drastic red shift for all three complexes. **1** exhibits a structureless band at 637 nm, and **2** and **3** show a structured feature with vibronic progression spacing of about 1100 nm. In addition, the emission energy exhibits a slight red shift for **2** in the concentration region of 6.8×10^{-5} mol/L to 5.1×10^{-4} mol/L, while **3** exhibits a slight blue shift in emission energy. The excitation spectra of these complexes measured at different concentrations also manifest concentration dependence (shown in Supporting Information). At lower concentrations ($<6.0 \times 10^{-5}$ mol/L), the band in the UV region dominates. With increased concentration ($> 6.0 \times 10^{-5}$ mol/L), a new band in the visible region (400−500 nm) appears, and this band becomes dominant for **2** and **3**. The trend discovered at 77 K is in accordance with that observed at room temperature. These concentration dependence studies clearly demonstrate that the degree of $\pi-\pi$ and metal−metal interactions can be adjusted by varying the complex concentration for these binuclear complexes. Especially for **1**, the concentration change can transform the emission from a ^{3}MLCT state at low concentrations to a $^3[d\sigma^*,\pi^*]$ state at high concentrations.

The emission lifetimes of these complexes at room temperature and 77 K have also been examined using the kinetic mode of the Edinburgh LP920 laser flash photolysis spectrometer, and the results are presented in Table 2. At room temperature, for complex concentration of $1.2-1.4 \times 10^{-4}$ mol/L, **1** and **2** exhibit monoexponential decay, with a lifetime of 0.20 μs for **1** and 1.50 μs for **2**. In contrast, **3** exhibits biexponential decays at a similar concentration, with a longer lifetime of 1.96 μs (68%) and a shorter one of 0.39 μs (32%). The time-resolved emission spectra (see Supporting Information) coincide with the lifetime measurement. The appearance of monoexponential decay for **1** and **2** implies the presence of a single emitting species at the complex concentration of $\sim 1.3 \times 10^{-4}$ mol/L, while the biexponential decay for **3** can be presumably attributed to a triplet−triplet annihilation. At 77 K, all three complexes (at concentrations of $1.2-1.4 \times 10^{-4}$ mol/L) exhibit biexponential decays, with a lifetime of 2.37 μs (89%) and 0.19 μs (11%) for **1**; 3.41 μs (92%) and 0.31 μs (8%) for **2**; and 8.24 μs (96%) and 0.57 μs (4%) for **3**. It is observed that the emission lifetimes at both room temperature and 77 K become longer when the concentration is increased to higher than 6.0×10^{-5} mol/L, which is consistent with the changes of the origin of the emitting state and/or degree of $\pi-\pi$ interactions when the concentration varies, as described earlier for the emission energy at different concentrations.

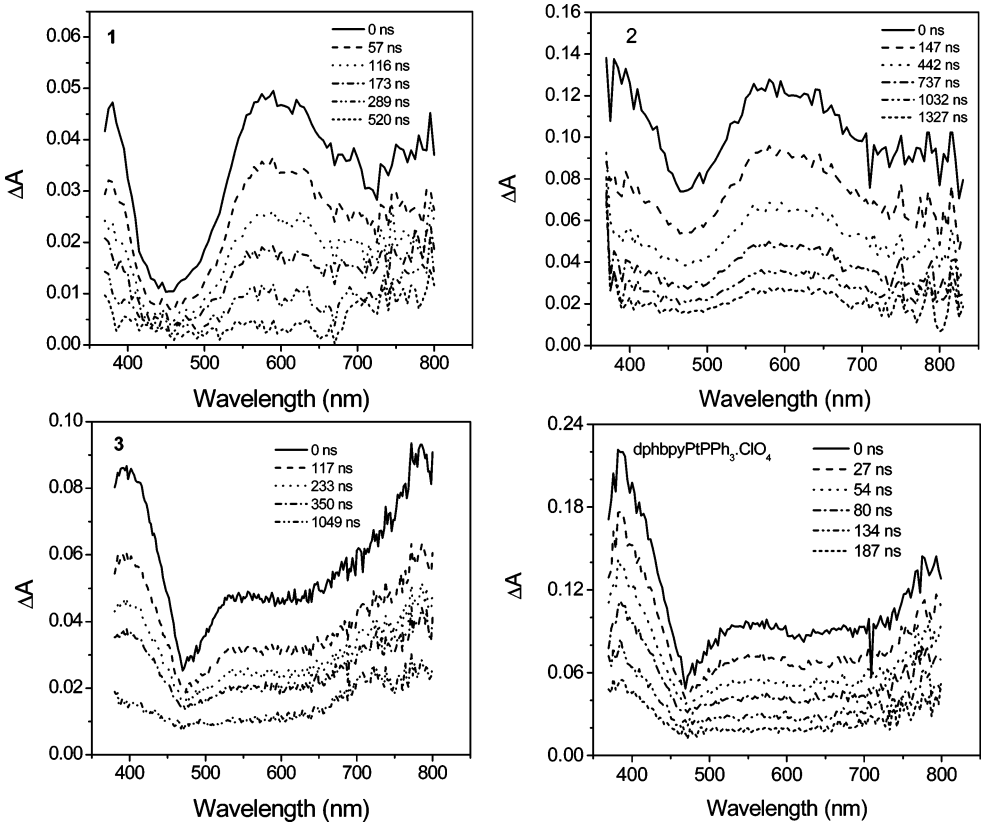

Figure 6. Time-resolved triplet transient difference absorption spectra of **1**−**3** and mononuclear platinum(II) triphenylphosphine complex (dphbpyPtPPh$_3$·ClO$_4$) in argon-degassed acetonitrile solutions at room temperature following 355 nm excitation. The time indicated in the figures is the time delay after the laser pulse. The complex concentration is 2.7×10^{-5} mol/L for **1**, 6.8×10^{-5} mol/L for **2**, 1.9×10^{-5} mol/L for **3**, and 7.5×10^{-5} mol/L for dphbpyPtPPh$_3$·ClO$_4$. The measurements were conducted in a 1-cm cuvette.

To determine the quantum yield of emission for these complexes, a comparative method was used,[10] in which a degassed aqueous solution of $[Ru(bpy)_3]Cl_2$ ($\phi_{em} = 0.042$)[11] was used as the reference and the samples were excited at 436 nm. The emission quantum yield is found to be 0.022 for **1**, 0.182 for **2**, and 0.032 for **3**. It is apparent that the emission quantum yield of **2** is more than 8 times as large as that of **1**, while the yield for **3** is comparable to that of its binuclear 6-phenyl-2,2′-dipyridine relative.[6d]

Transient Difference Absorption. As discussed earlier for the UV−vis spectra, **1**−**3** are essentially transparent in the visible to the near-IR region even at high concentrations, providing a broad optical window for nonlinear absorption and optical limiting to occur.[8] Emission studies have revealed that these complexes possess a relatively long-lived triplet excited state at high concentrations. Therefore, broadband triplet excited-state absorption is expected in the visible to the near-IR region. To demonstrate this, triplet transient difference absorption spectra were measured using an Edinburgh LP920 laser flash photolysis spectrometer. As displayed in Figure 6 for **1**−**3** and their mononuclear triphenylphosphine congener, these complexes exhibit a positive absorption band from 370 to 800 nm with a narrow band in the near-UV and two broad, moderately intense absorption bands in the visible and extending to the near-IR region, implying a stronger triplet excited-state absorption than that of the ground state from the near-UV to the near-IR region. To the best of our knowledge, this is the broadest positive transient absorption band reported to date. It is noticeable that the short-wavelength band maxima red-shift with the increased bridging length, varying from 380 nm for **1** to 385 nm for **2** and 390 nm for **3**; while the low energy band blue-shifts from 590 nm for **1** to 571 nm for **2** and 536 nm for **3**. The lifetimes measured at different wavelengths for each complex are all similar, indicating that the absorption bands all arise from the same transient species. In addition, the lifetimes obtained from the kinetic transient absorption measurement coincide with those from the emission measurements, suggesting that the transient absorption arises from the same excited state that emits, that is, from a state that possesses ^{3}MLCT character for **2** and **3** and $^3[d\sigma^*,\pi^*]$ (^{3}MMLCT) for **1**. Or alternatively, the absorbing excited state is in equilibrium with the emitting excited state. The transient absorption in the visible to near-IR region likely arises from the dphbpy anion radical that is present in the ^{3}MLCT state and the $^3[d\sigma^*,\pi^*]$ (^{3}MMLCT) state. This notion can be supported by the similar feature of the spectra for **1**−**3** to that of their mononuclear triphenylphosphine counterpart and is in line with the transient absorptions of diimine platinum(II) bis-acetylide complexes[12] and the mononuclear platinum(II) terpyridyl complexes,[5b] in which the transient species giving rise to the transient absorption spectra is attributed to the diimine or terpyridyl anions.

(10) Demas, J. N.; Crosby, G. A. *J. Phys. Chem.* **1971**, *75*, 991.
(11) Van Houten, J.; Watts, R. J. *J. Am. Chem. Soc.* **1976**, 4853.
(12) Whittle, C. E.; Weinstein, J. A.; George, M. W.; Schanze, K. S. *Inorg. Chem.* **2001**, *40*, 4053.

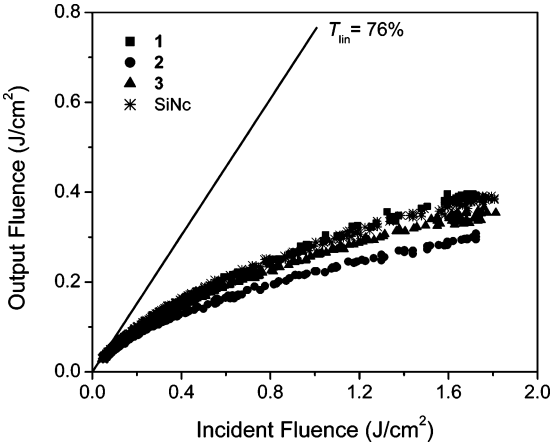

Figure 7. Optical limiting curves for **1**−**3** at 532 nm for 4.1 ns laser pulses. The linear transmission for all samples was adjusted to 76% in a 2-mm cuvette. **1** and **2** were dissolved in CH_3CN, **3** was dissolved in DMSO, and SiNc was dissolved in CH_2Cl_2.

Table 3. Optical Limiting Parameters for Complexes 1−3 at a Linear Transmittance of 76%

complex	σ_0[a] (cm^2)	F_{th}[b] (J/cm^2)	$F_{through}$[c] (J/cm^2)	T_{nonlin}[d]	σ_{eff}/σ_0
1[e]	8.9×10^{-19}	0.102	0.39	0.23	>5.35
2[e]	9.1×10^{-20}	0.075	0.29	0.17	>6.46
3[f]	6.1×10^{-20}	0.108	0.34	0.20	>5.86
SiNc[g]	8.0×10^{-18}	0.135	0.38	0.22	>5.52

[a] Ground-state absorption cross section at 532 nm. [b] Limiting threshold, defined as the incident fluence at which point the transmittance drops to 70% of the linear transmission. [c] Maximum output fluence at an incident fluence of 1.7 J/cm^2. [d] Nonlinear transmittance at an incident fluence of 1.7 J/cm^2. [e] **1** and **2** were dissolved in CH_3CN. [f] **3** was dissolved in DMSO. [g] SiNc was dissolved in CH_2Cl_2.

Optical Limiting. As a result of the broad and relatively intense triplet excited-state transient absorption and the long triplet excited-state lifetime, reverse saturable absorption could occur at a broad spectral region, which would be very useful for optical limiting of nanosecond laser pulses.[8] To demonstrate this, nonlinear transmission measurements were carried out at 532 nm using a 4.1 ns (fwhm) Nd:YAG laser. The results are manifested in Figure 7 and Table 3. It is quite clear that among the three binuclear complexes, **2** exhibits the best optical limiting, with a limiting threshold (defined as the incident fluence at which point the transmittance drops to 70% of the linear transmittance) of 0.075 J/cm^2. The transmittance decreases to 17% at an incident fluence of 1.7 J/cm^2, a 78% drop in comparison to the linear transmission. Both limiting threshold and limiting throughput for **2** are lower than those of SiNc, one of the most promising optical limiting materials reported in the literature.[13] The lower limiting threshold and limiting throughput in conjunction with the much broader triplet transient absorption suggest that **2** should be a better broadband optical limiting material than SiNc. **3** also shows a lower limiting threshold and limiting throughput than those of SiNc, while **1** manifests a lower limiting threshold but comparable limiting throughput to those of SiNc. The better optical limiting performances of **2** and **3** than that of **1** are likely due to the much weaker ground-state absorption of **2** and **3** at 532 nm, which in turn

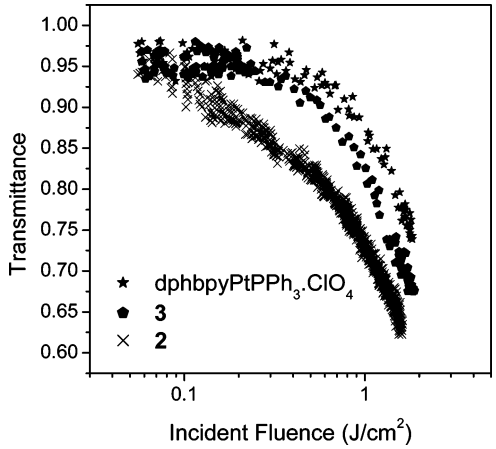

Figure 8. Optical limiting curves for the mononuclear platinum(II) triphenylphosphine complex ($dphbpyPtPPh_3.ClO_4$) and complexes **2** and **3** for 4.1 ns laser pulses at 532 nm in a 2-mm cell. $dphbpyPtPPh_3{\cdot}ClO_4$ was dissolved in CH_2Cl_2, and **2** and **3** were dissolved in CH_3CN. The linear transmission was adjusted to 96%.

increases the ratio of the excited-state absorption cross section to the ground-state absorption cross section, giving rise to an enhanced optical limiting. In addition, the much longer excited-state absorption lifetimes of **2** and **3** could also play a role in their enhanced optical limiting performances.

To further demonstrate whether the better optical limiting performances of these binuclear complexes originate from the intramolecular metal−metal or $\pi-\pi$ interactions, the optical limiting of the mononuclear congener has been studied and is compared to those of **2** and **3**, which essentially show no intramolecular metal−metal interactions, and the results are presented in Figure 8. As a result of the very low linear absorption for these complexes at 532 nm and the solubility limit in CH_2Cl_2 for the mononuclear complex, the comparison was performed in solutions with a linear transmittance of 96%. It is apparent that **2** and **3** exhibit a better optical limiting performance than that of the mononuclear complex even though none of them shows metal−metal interactions. The stronger optical limiting of **2** and **3** is presumably associated with the much longer triplet excited-state lifetime of these two complexes in comparison to that of the mononuclear species (∼110 ns) even at a relatively dilute concentration ($\sim 1 \times 10^{-5}$ mol/L).

To quantitatively compare the optical limiting performances, a figure of merit $\sigma_{eff}/\sigma_0 = \ln T_{sat}/(\ln T_{lin})$[14] is used, where σ_{eff} is the effective excited-state absorption cross section, σ_0 is the ground-state absorption cross section, T_{sat} is the transmittance at the saturation fluence (defined as $F_{sat} = h\nu/\sigma_0\Phi_t$, where σ_0 is the ground-state absorption cross section, and Φ_t is the quantum yield of the first triplet excited state),[14] and T_{lin} is the linear transmittance. As a result of the limitation of the damage threshold of the quartz cell (5 J/cm^2), it was unable to reach the saturable transmittance at the maximum incident fluence (1.7 J/cm^2) used in our experiment. However, the lowest transmittance at the highest incident fluence can be used to calculate the lower bound of σ_{eff}/σ_0 for these complexes. The results are listed in Table

(13) Mansour, K.; Alvarez, D., Jr.; Perry, K. J.; Choong, I.; Marden, S. R.; Perry, J. W. *Proc. SPIE* **1993**, *1853*, 132.

(14) Perry, J. W.; Mansour, K.; Marder, S. R.; Perry, K. J.; Alvarez, D., Jr.; Choong, I. *Opt. Lett.* **1994**, *19*, 625.

3. It is obvious that this value is higher for **2** and **3** than that of SiNc.

It is worthy of mention that although the optical limiting effect of the binuclear cyclometalated platinum(II) complexes reported in this paper is the first report for this series of complexes, the nonlinear optical effect of other binuclear transition-metal complexes, such as diruthenium complexes, have been reported in the literature.[15,16] To compare the nonlinear optical effect of the binuclear platinum(II) complexes to those of the ruthenium complexes, the imaginary part of the third-order susceptibility $\mathrm{Im}(\chi^{(3)})$ (m^2/V^2) that is related to the nonlinear absorption has been estimated for the platinum(II) complexes using the following equation:[17]

$$\mathrm{Im}(\chi^{(3)}) = \frac{\epsilon_0 c n_0 \lambda N_A C(\sigma_{ex} - 2\sigma_0)}{16\pi I_{sat}} \quad (1)$$

where ϵ_0 is the vacuum dielectric constant, c is the speed of light, n_0 is the linear refractive index of the solution, λ is the laser wavelength, N_A is the Avogadro's constant, C is the molar concentration, σ_{ex} and σ_0 are the excited-state and ground-state absorption cross sections, respectively, and I_{sat} is the saturation intensity at $T_{sat} = (T_0 T_{ex})^{1/2}$, with T_0 and T_{ex} being the linear transmission and the transmission at the highest incident fluence. Applying the lower bound σ_{eff}/σ_0 values shown in Table 3 and the I_{sat} values found from the experimental curves to eq 1, the lower bound $\mathrm{Im}(\chi^{(3)})/C$ value was estimated to be 7.4×10^{-8} esu/M for **1**, 9.3×10^{-9} esu/M for **2**, and 4.6×10^{-9} esu/M for **3** at 532 nm. These values are comparable or even larger than some of the $\chi^{(3)}/C$ values reported for diruthenium complexes with an oligoyne tail measured by the degenerate four-wave mixing (DFWM) technique at 532 nm using a nanosecond laser.[15] Taking into account the fact that DFWM technique measures the contributions from both nonlinear absorption and nonlinear refraction, and a significant thermal effect contributes to the $\chi^{(3)}$ values of samples with considerable linear absorption when DFWM measurement is carried out using a nanosecond laser, it is not surprising that $\chi^{(3)}/C$ values for some of the diruthenium complexes with an oligoyne tail is larger than the lower bound value of the $\mathrm{Im}(\chi^{(3)})/C$ value for complexes **1**−**3**. Nevertheless, it is particularly important to realize that a larger $\chi^{(3)}$ value does not necessarily indicate a strong optical limiting, which has been demonstrated by complexes **2** and **3** that possess a lower $\mathrm{Im}(\chi^{(3)})/C$ value but a stronger optical limiting than that of **1**. This notion is further supported by the tetrakis(2,2′-dipyridyl)diruthenium complexes, which exhibit large resonant third-order susceptibility ($\chi^{(3)}/C \sim 5.4 \times 10^{-10}$ esu/M − 8.4×10^{-9} esu/M) but show very weak optical limiting for nanosecond laser pulses (transmission drops from 89% of linear transmittance to 80% at incident fluence of 2.3 J/cm^2) and saturable absorption for picosecond laser pulses.[16] Therefore, for optical limiting based on reserve saturable absorption, it is most important to evaluate and compare the σ_{eff}/σ_0 value for different systems rather than using the $\chi^{(3)}$ value.

Conclusion

The two new binuclear cyclometalated platinum(II) complexes **2** and **3** exhibit negligible metal−metal interactions between the two platinum centers. Both complexes emit at room temperature in CH_3CN solution and at 77 K glass with relatively long lifetimes (μs), which can be ascribed to a ^{3}MLCT excited state. **2** exhibits a relatively high emission efficiency (0.182), and the emission profiles show concentration dependence. With increased concentration, the emission band becomes broader and red-shifts, presumably due to $\pi-\pi$ interactions between the two [PtL] units. In addition, both complexes possess very broad positive transient difference absorption bands from the near-UV and extending to the near-IR spectral region. The nonlinear transmission experiment at 532 nm demonstrates that they exhibit better optical limiting for nanosecond laser pulses than that of SiNc. The high emission quantum yield, relatively long excited-state lifetime, broadband excited-state absorption, and excellent optical limiting performance at 532 nm for **2** and **3** suggest that these complexes could be very promising candidates for organic light-emitting devices (OLED) and broadband optical limiting applications.

Acknowledgment. Acknowledgment is made to the Donors of the American Chemical Society Petroleum Research Fund (no. 38243-G3) and National Science Foundation CAREER Award (CHE-0449598) for financial support. The authors thank the North Dakota EPSCoR (EPSCoR Seed Award, Instrumental Award, and Faculty Start-up Award) for support.

Supporting Information Available: Concentration-dependent excitation profiles at 77 K and time-resolved emission spectra at room temperature and 77 K (PDF). This material is available free of charge via the Internet at http://pubs.acs.org.

CM060161N

(15) Xu, G.-L.; Wang, C.-Y.; Ni, Y.-H.; Goodson, T. G., III; Ren, T. *Organometallics* **2005**, *24*, 3247.
(16) Sun, W.; Patton, T. H.; Stultz, L. K.; Claude, J. P. *Opt. Commun.* **2003**, *218*, 189.
(17) Henari, F.; Callaghan, J.; Stiel, H.; Blau, W.; Cardin, D. J. *Chem. Phys. Lett.* **1992**, *199*, 144.